Comprehensive Journal of Science
Volume (11), Issue (41), (JUNE, 2026)
ISSN: 3014-6266

مجلة العلوم الشاملة
المجلد (11) العدد 41 يونيو 2026
ردمد: 3014-6266

Kinetic Analysis of Lead Removal from Industrial Wastewater Using an Anionic Surfactant

Fouad Sadig Rashed[1] and Akram Mohamed Aljamah

[1]Chemical Engineering Department, College of Engineering, Sabratha University, Libya.
Email: fouad.rashed@sabu.edu.ly
[2]Architectural Engineering Department, High Institute of Science and Technology, Zawia, Libya.
Email: aljama.akram@gmail.com

تاريخ الاستلام:2026/4/03 –تاريخ المراجعة:2026/05/04– تاريخ القبول: 2026/05/16– تاريخ للنشر2026/06/03

Abstract:

The release of untreated industrial wastewater, particularly when it contains heavy metals, significantly harms the aquatic environment. Among these metals, lead is recognized as one of the toxic heavy metals commonly found in industrial effluents. Elevated levels of lead in water can lead to various physiological and health issues in humans and other organisms. Research was conducted on the flotation kinetics of lead using sodium dodecyl sulfate, anionic collector. Study the prediction of lead separation kinetics from wastewater using ion flotation is critically important for several interconnected reasons; predictable, scalable, and economical engineering solution. The study explored chemical kinetics by examining key parameters such as wastewater pH and collector concentration. Time–recovery data for lead flotation were analyzed using a first–order equation for flotation kinetics $R_t = R_\infty \left(1 - e^{-kt}\right)$, which allowed for the calculation of the flotation rate constant and the cumulative recovery at infinity (R_∞). The experimental results showed acceptable alignment with the first–order kinetic model. Results showed that the adsorption rate increased with initial SDS concentration from 25 to 100 mg/L, with the highest reaction rate observed at 100 mg/L (k = 0.0707 min^{-1}). Correlation coefficients (R^2) confirmed acceptable linear relationships with consistent negative slopes across all data groups. For pH experiments conducted at constant initial SDS concentration (50 mg/L) across pH values of 3, 5, and 8, adsorption increased with rising pH up to an optimum at pH 5 (k = 0.0229 min^{-1}), after which it decreased at pH 8 (k = 0.0208 min^{-1}). The lowest reaction rate was observed at pH 3 (k = 0.0138 min^{-1}). Cumulative recovery values ranged from 56.10% to 89.52%, with the maximum recovery (89.52%) achieved at 50 mg/L SDS concentration and pH 8. These findings demonstrate that both initial lead concentration and pH significantly influence the adsorption mechanism of SDS onto lead surfaces.

Keywords: Flotation, lead, Sodium Dodecyl Sulfate, Flotation Kinetics, first–Order Kinetics Model

1. Introduction:

The rapid expansion of industrial activities has significantly exacerbated the release of hazardous pollutants into aquatic environments, with heavy metals representing one of the most critical concerns due to their toxicity and persistence [1]. Unlike organic contaminants, heavy metals such as lead, chromium, and mercury are non-biodegradable, allowing them to persist in ecosystems for decades and accumulate through trophic pathways [2]. Their presence in industrial effluents—originating from sectors including mining, electroplating, and manufacturing—poses direct risks to both ecological integrity and human health, as chronic exposure has been linked to neurological damage, carcinogenesis, and metabolic disruption [3]. Consequently, effective remediation strategies, ranging from chemical precipitation to bioremediation, are essential for mitigating these risks before wastewater is discharged into receiving water bodies [4].

Among these toxic elements, lead (Pb) is particularly hazardous due to its high toxicity, environmental persistence, and tendency to bioaccumulate in living organisms [1]. Lead remains in ecosystems indefinitely, cycling through water, soil, and food chains [2]. Industrial activities, including battery manufacturing, mining, metal finishing, and chemical production, are primary contributors to lead-laden wastewater, which, if improperly treated, can contaminate drinking water sources and agricultural lands [5]. Chronic exposure to lead, even at low concentrations, is associated with irreversible neurological damage, cognitive impairment, and organ failure, with children and pregnant women being especially vulnerable [6]. In response to these risks, regulatory frameworks such as the U.S. Clean Water Act and the EU's Water Framework Directive mandate the removal of lead from industrial effluents prior to discharge [7]. Various maximum permitted levels of lead in the water are shown in **Table 1.1**.

Table 1.1: Various maximum permitted levels for lead metal composition [8].

Metal	unit	Permissible Limit		
		WHO	**USEPA**	**BIS: IS 3025**
Lead (Pd^{2+})	Mg/L	0.010	0.015	0.010

WHO: World Health Organization.
USEPA: U. S. Environmental Protection Agency.
BIS: Bureau of Indian Standard.

To achieve compliance, various treatment technologies—including chemical precipitation, ion exchange, adsorption, flotation, and membrane separation—have been developed and implemented [4]. Flotation, a technique originally developed in the mining industry, has now been widely adopted for wastewater treatment. It is commonly used to separate heavy metals from liquids through bubble attachment, a method derived from mineral processing. The technology is also becoming increasingly significant in hydrometallurgical applications, with ion flotation emerging as a key separation process for concentrating, recovering, and extracting metal ions from dilute aqueous solutions. The recovery or removal of metal ions from such solutions is a critical challenge across various scientific disciplines, particularly in scenarios involving low-concentration solutions. Successfully addressing this challenge offers substantial economic and environmental benefits for many industries [9].
This study aims to examining the kinetics of lead ions removal through a batch flotation process, utilizing sodium dodecyl sulfate (SDS) as an adsorbent agent. A first–order model was employed by Excel program to determine the optimal SDS concentration and pH levels.

2. Experimental work

2.1 Flotation Column

A laboratory-scale flotation column was designed and fabricated for experimental purposes. The schematic diagram of the experimental setup is presented in **Figure 2.1**. The flotation column was constructed using Pyrex glass, with an internal diameter of 8 mm, an external diameter of 0.12 mm, and a height of 120 cm.

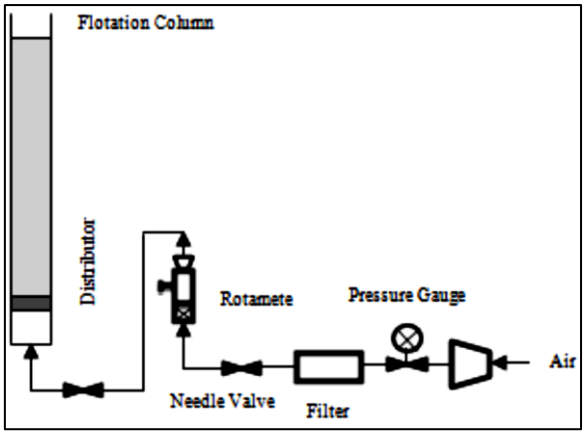

Figure 2.1: Schematic diagram of the experimental system

2.3 Working Procedure

The laboratory-scale flotation column, made of Pyrex glass as detailed earlier, was developed with dimensions of 8 mm internal diameter, 0.12 mm external diameter, and 120 cm height. Air was supplied to the flotation column via a compressor and regulated using a pre-calibrated rotameter. The air, introduced at the bottom of the column, was dispersed into the liquid as fine bubbles. The feed material was gently introduced at the top of the column. During operation, the column was pressurized to prevent liquid seepage through the perforations. A perforated air distributor was positioned at the bottom of the column for effective bubble dispersion. This distributor contained 20 holes with a diameter of 0.1 cm each, arranged in an equilateral triangular pattern throughout its surface area. The column was operated in batch mode for the liquid phase and in continuous flow mode for the air phase. All experimental procedures were carried out at a constant ambient laboratory temperature.

3. Flotation Kinetics

Various methods are utilized to determine the order and rate constant of flotation in metals, including computational and graphical approaches. These methods are fundamentally based on the law of mass action, which asserts that the rate of a chemical reaction is proportional to the active masses of the reacting substances at any given moment. When applying this law to metal flotation, terms specific to flotation replace those used in chemical reactions. Specifically, "flotation" substitutes "chemical reaction," and the "floatable amount of metal" replaces "active masses of reactants." Several physical variables influence the flotation rate. However, when external factors such as the liquid volume in the flotation process and the aeration rate are maintained at constant levels, the flotation rate can be expressed as follows [10]:

$$rate = \frac{dC}{dt} = -kC^n \qquad \rightarrow (1)$$

$$-\frac{dC}{dt} = kC^n \qquad \rightarrow (2)$$

Where:

C: Concentration of the floatable metal at time t.
k: Rate constant.
n: Reaction order.

Since flotation typically follows first-order kinetics, the reaction order (n) is equal to 1. Substituting this value into Equation (2) modifies it to [11]:

$$-\frac{dC}{dt} = kC \qquad \rightarrow (3)$$

By integrating Equation (3) within set limits:

$$-\int_{C_0}^{C} dC = k\int_{0}^{t} dt \qquad \rightarrow (4)$$

We derive the logarithmic form of the integrated rate law for a first-order reaction:

$$\ln\frac{C_0}{C_t} = kt \qquad \rightarrow (5)$$

This can also be expressed as:

$$\ln C_t = \ln C_0 - kt \qquad \rightarrow (6)$$

Equation (5) is further rearranged into an exponential form:

$$\frac{C_0}{C_t} = e^{kt} \qquad \rightarrow (7)$$

Or rewritten as:

$$C_0 - C_t = C_0\left(1 - e^{-kt}\right) \qquad \rightarrow (8)$$

Where: C_0: Initial concentration of the metal at time zero (t = 0, C = C_0), also referred to as the maximum theoretically floatable quantity or the maximum possible recovery. However, complete recovery of the metal in the liquid phase is rarely achieved due to factors such as unfloatable particles like very coarse ones. To account for this, the term C_0 in Equation (8) is replaced with R_∞, which represents the maximum achievable recovery or cumulative recovery at infinite time. Additionally, the term on the left-hand side of Equation (8), ($C_0 - C_t$), represents the cumulative recovery at time t. Incorporating these changes, Equation (8) evolves into:

$$R_t = R_\infty\left(1 - e^{-kt}\right) \qquad \rightarrow (9)$$

Where:

R_t: Cumulative recovery at time t.
R_∞: Maximum achievable recovery outlined by the system's constraints.

4. Results and Discussion

To determine the reaction rate constant (k), equation (4) was utilized plotting (ln C_t) against time (t). this yielded a straight line with a slope of (– k), which was derived using a statistical program to analyze the slopes of these lines. Additionally, equation (9) was employed for calculating the cumulative recovery. The values of the reaction rate constants, correlation coefficients, and cumulative recovery are presented in **Tables 4.1** and **4.2**. calculations for (k) were performed for all data points a cross varying conditions, with results depicted in **Figures 4.1** to **4.6** for each initial concentration and set of optimal parameters. The correlation coefficients (R^2) in **Tables 4.1** and **4.2** confirm an acceptable linear relationship with a consistent negative slope across the data groups. In the first of the three figures, the adsorption rate shows an increases as the initial concentration rises from 25 to 100 mg/L. as detailed in **Table 4.1**, the experiment with an initial lead concentration of 100 mg/L exhibited the highest reaction rate.

Additional experiments were conducted at varying pH levels of 3, 5, and 8, utilizing sodium dodecyl sulfate solutions with a consistent initial concentration of 50 mg/L. The corresponding experimental

results are detailed in **Table 4.2**. The impact of pH on the adsorption of sodium dodecyl sulfate onto lead surfaces is illustrated through **Figure 4.4** to **4.6**. The data reveal that adsorption increases with rising pH, reaching a peak at pH 5, after which it starts to decrease. Overall, the findings indicate that the adsorption mechanism of sodium dodecyl sulfate on lead is influenced by both the initial lead concentration and pH level.

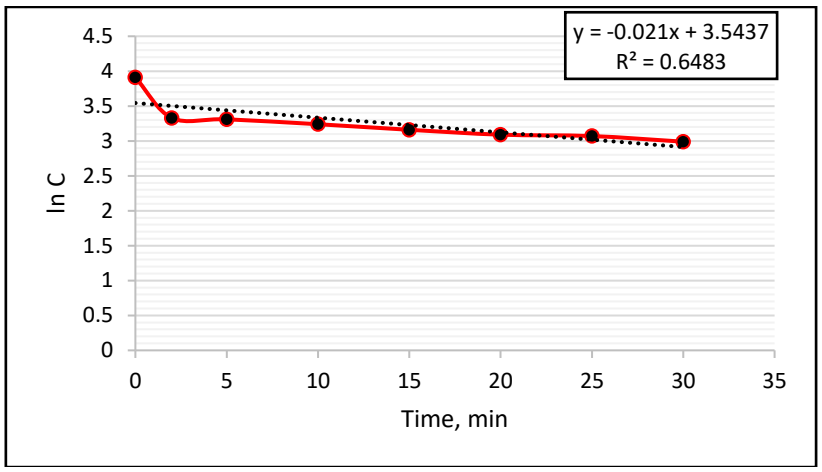

Figure 4.1: First–order reaction curve illustrating the kinetics of sodium dodecyl sulfate adsorption on the lead surface at an SDS concentration is 25 mg/L.

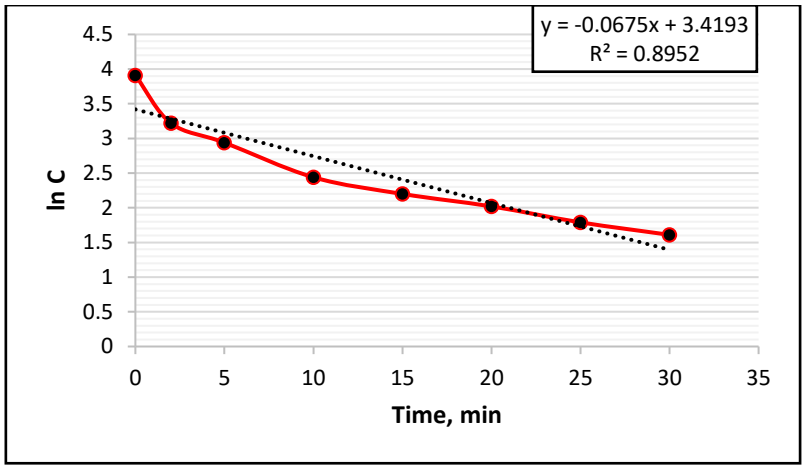

Figure 4.2: First–order reaction curve illustrating the kinetics of sodium dodecyl sulfate adsorption on the lead surface at an SDS concentration is 50 mg/L.

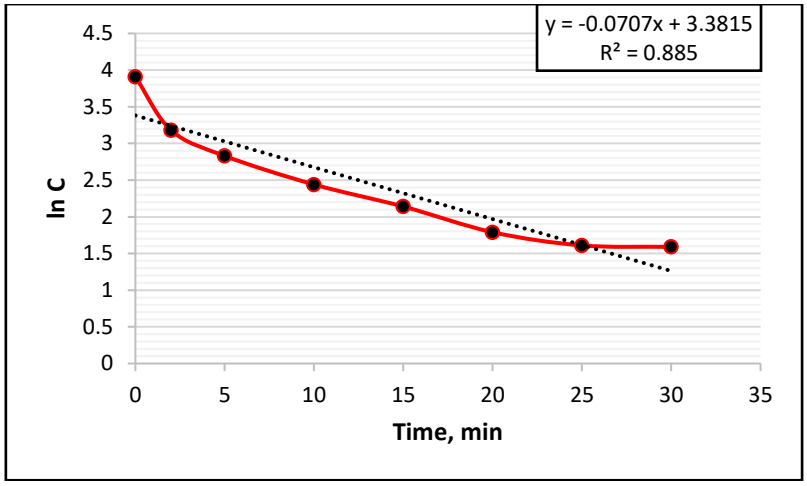

Figure 4.3: First–order reaction curve illustrating the kinetics of sodium dodecyl sulfate adsorption on the lead surface at an SDS concentration is 100 mg/L.

Table 4.1: Illustrates the first – order reaction kinetics of SDS adsorption on a lead surface at different concentrations. The initial lead concentration is 50 mg/L and pH level is maintained at 8.

SDS mg/L	k min^{-1}	R^2	R_t
25	0.0453	64.83	
50	0.0509	89.52	
100	0.0707	88.50	

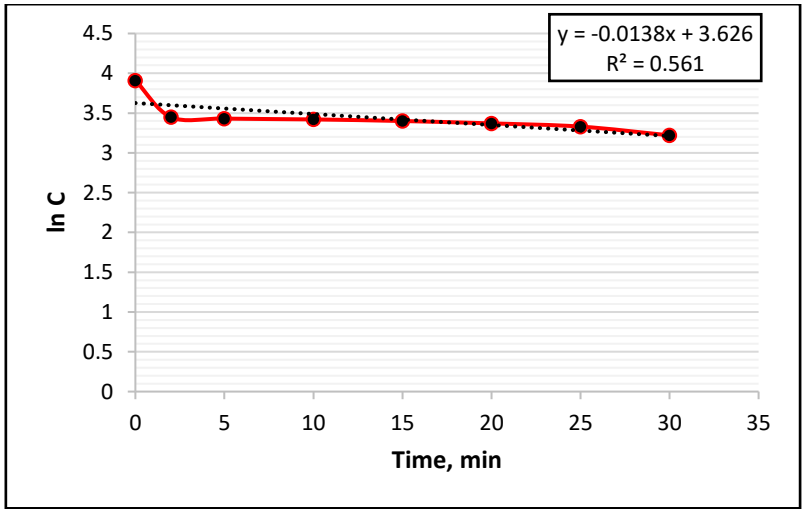

Figure 4.4: First–order reaction illustrating the kinetics of SDS adsorption on the lead surface, conducted at an initial concentration is 50 mg/L and a pH of 3.

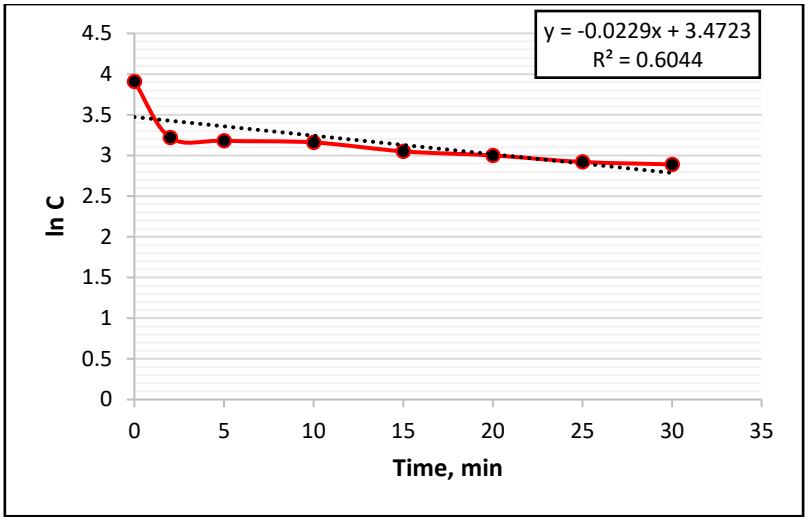

Figure 4.5: First–order reaction illustrating the kinetics of SDS adsorption on the lead surface, conducted at an initial concentration is 50 mg/L and a pH of 5.

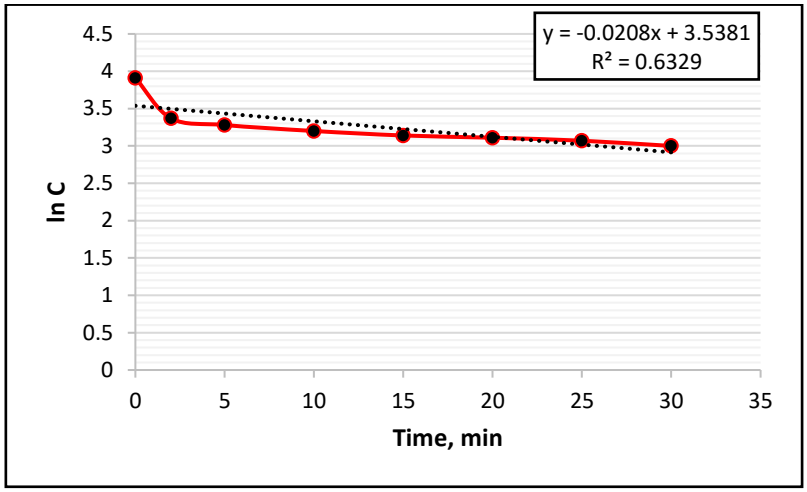

Figure 4.4: First–order reaction illustrating the kinetics of SDS adsorption on the lead surface, conducted at an initial concentration is 50 mg/L and a pH of 8.

Table 4.2: Illustrates the first – order reaction kinetics of SDS adsorption on a lead surface at different concentrations. The data represents an initial SDS concentration of 50 mg/L with different pH levels.

SDS mg/L	k min^{-1}	R^2	R_t
3	0.0138	56.10	
5	0.0229	60.44	
8	0.0208	63.29	

5. Conclusion

Kinetics adsorption experiments were carried out to analyze the adsorption behavior of the anionic agent sodium dodecyl sulfate. The consumption rate of sodium dodecyl sulfate serves as an indicator of the amount adsorbed or the degree of conditioning achieved. It was observed that the reaction rate constant remains unaffected by the collector concentration, with k values showing consistency across different experimental concentrations. However, the effect of pH on the reaction rate proved to be highly

significant. The experimental kinetics data also demonstrated the potential to predict lead floatability. Additionally, it highlights the need to establish relationships between various parameters and performance during the conditioning stage in ion flotation and adsorption kinetics, enabling the optimization of both selectivity and recovery of the target metal.

References:

1. Tchounwou, P. B., Yadjou, C. G., Patlolla, A. K., and Sutton, D. J., *Heavy metal toxicity and the environment*, Molecular, Critical and Environmental Toxicology, 101, 133–164, 2012.
2. Jaishanker, M., Testen, T., Anbalagan, N., Mathew, B. B., and Beeregowda, K. N., *Toxicity, mechanism and health effects of some heavy metals*, Interdisciplinary Toxicology, 7(2), 60–72, 2014.
3. Ali, H., Khan, E., and Ilahi, I., *Environmental chemistry and ecotoxicology of hazardous heavy metals: environmental persistence, toxicity, and bioaccumulation*, Journal of Chemistry, 1–14, 2019.
4. Fu, F. and Wang, Q., *Removal of heavy metal ions from wastewater: A review*, Journal of Environmental Management, 92(3), 407–418, 2011.
5. U. S. Environmental Protection Agency (EPA), *Effluent Guidelines: Lead manufacturing*, Washington, DC: EPA, 2021.
6. World Health Organization (WHO), *Lead poisoning and health*, Geneva: WHO, 2019.
7. European Commission, *Directive 2000/60/EC of the European Parliament and of the Council establishing a framework for Community action in the field of water policy*, Official Journal of the European Communities, L327, 1–73, 2000.
8. Jamom, A. M., & Albohli, N. A. (2026). Evaluation of the technical and environmental feasibility of replacing a steam generation unit with wind turbines at the Zawia refinery, Libya. *Al-Farooq Journal of Sciences*, *2*(3), 149-160.
9. Hoseinian F., Safari M., and Deglon, *Ion flotation kinetic predictions using empirical and phenomenological*, Minerals Engineering, 210, 2024.
10. Fatma, A. and Gullay B., *Ion flotation and its applications on concentration, recovery, and removal of metal ions from solutions*, Physicochemical Problems of Mineral Processing, 58(5), 1–19, 2022.
11. Rezaei R., Mirghaffari N., and Rezaei B., *Kinetic Isotherms Study of Copper Adsorption from Solutions by a Low–Cost Adsorbent*, International Journal of Chemical and Environmental Engineering, 3(4), 225–229, 2012.
12. Alnnale, T. (2026). Predictive Governance in Digital Enterprises: An LSTM-Enhanced Deep Learning Framework for Economic Optimization of IT Incident Management Using Enriched Process Logs. Al-Farooq Journal of Sciences, 2(3), 86-113.
13. Aksu Z., and Isoglu I., *Removal of copper (II) ions from aqueous solution by biosorption onto agriculture waste sugar beet pulp*, Process Biochem, 40, 3031–3044, 2005.